Picosecond Studies of Optical Second Harmonic Generation in Atomic Vapor

Christopher S. Mullin, Doseok Kim, Marla B. Feller, and Y. R. Shen
Department of Physics, University of California, Berkeley, California 94720-7300
Materials Sciences Division, Lawrence Berkeley Laboratory, Berkeley, California 94720-7300
(Received 26 July 1994)

Picosecond laser pulses are used to study the forbidden resonant second harmonic generation (SHG) in atomic vapor. The results can be understood quantitatively by an ionization-initiated dc-field-induced SHG model taking into account the temporal buildup of the dc field and transient behavior of the two-photon coherent excitation of the vapor.

PACS numbers: 42.65.Ky, 32.80.Wr, 42.50.Md

Second harmonic generation (SHG) in atomic vapor is a highly forbidden nonlinear optical process. Microscopically, the second-order polarizability for an atom should vanish in the electric-dipole approximation [1]. Macroscopically, SHG in bulk isotropic media is forbidden to all multipole orders in the plane–wave approximation [2]. Yet many experiments in the past have demonstrated that SHG in alkali or alkali-earth vapors can be easily detected when an exciting laser pulse is tuned to a two-photon resonance [3,4]. This is true even if the resonance is an $s \rightarrow s$ transition, with which no resonant emission can be expected since all its multipole matrix elements should be identically zero. Clearly, in those experiments, the symmetry of the medium must have been broken during the laser excitation. Several mechanisms have been proposed to provide the required broken symmetry [3–5]. The most plausible one is that of laser-induced resonant ionization followed by dc-field-induced SHG [3,5]. Indeed, Stoicheff and co-workers have recently shown that this model explains their results of resonant SHG in atomic hydrogen vapor very well [6]. One would expect that it should take a finite amount of time for the dc field to build up from laser ionization, and therefore the observed SHG should vary on the same time scale. However, in essentially all experiments, nanosecond laser pulses were used and they may not have the needed time resolution. To probe the time-varying dc field that induces the SHG, a picosecond pump laser pulse should be employed. Nonresonant SHG experiments in atomic vapor with picosecond laser pulses have been reported earlier [7]. They used pump intensities several orders higher than in the earlier case, and the results of the two cases are expected to be very different. This paper reports the first detailed study of picosecond resonant SHG in an atomic vapor. We have found, surprisingly, that even a picosecond excitation pulse can generate an easily detectable SH signal although the buildup time of the dc field from laser ionization is of the order of 100 ps. This result, however, can be understood if we realize that the short laser pulse can induce, by two-photon resonance, a coherent excitation in the vapor with a dephasing time also of the order of 100 ps [8]. Coherent emission of this coherent excitation in the vapor is forbidden, but becomes allowed in the presence of the dc field. Using the pump-probe scheme, we have actually observed the time-varying SHG resulting from the dc-field-induced emission of coherent excitation. Theoretical calculations based on the above picture yield a semiquantitative agreement with experiment.

Our experiment was carried out in a potassium/argon mixture inside a heat pipe. The potassium vapor pressure was kept at 0.6 Torr, and the argon pressure was allowed to vary from 5 to 100 Torr. Amplified 2 ps dye laser pulses with a 10 Hz repetition rate and ~200 μJ/pulse were used as the pump pulses. These pulses were tuned to the two-photon resonant $4s$-$9d$ transition of potassium at 2978.7 Å where a peak SHG was observed. Similar results were found when the laser pulses were tuned to the two-photon transitions of $4s$-$11s$, $4s$-$10d$, etc. The SH signal was detected by a photon-counting detection system after being properly filtered through a double monochromator with a 1 Å resolution. With the laser beam focused to a beam radius of 300 μm and a peak intensity of 10^{10} W/cm^2 over a length of 10 cm in a K(0.6 Torr)/Ar(20 Torr) mixture, the observed SH signal was ~100 photons/pulse. Figure 1 shows the measured SHG as a function of pump intensity at the Ar pressure of 20 Torr. It exhibits an I^8 dependence at low pump intensities and saturates at 10^{10} W/cm^2. This differs from observations with nanosecond pulses where the pump intensity dependence was typically I^2 before it saturated [3,4]. The SH output in our experiment was found to be collimated to within 1 mrad. The intensity distribution had two symmetric lobes in the direction of the input beam polarization. The overall polarization of the SH output was predominantly parallel to that of the fundamental input. We have also measured SHG as a function of Ar pressure with two different laser intensities. The result is presented in Fig. 2. The SHG signal decreases rapidly with the increase of Ar pressure, much more rapidly than that observed with nanosecond pump pulses [4].

We can understand the above results using the ionization-initiated dc-field-induced SHG model. In our case, ionization of K was dominated by a three-photon process. The dc field E_{dc} generated by electrons diffusing

 0031-9007/95/74(14)/2678(4)$06.00

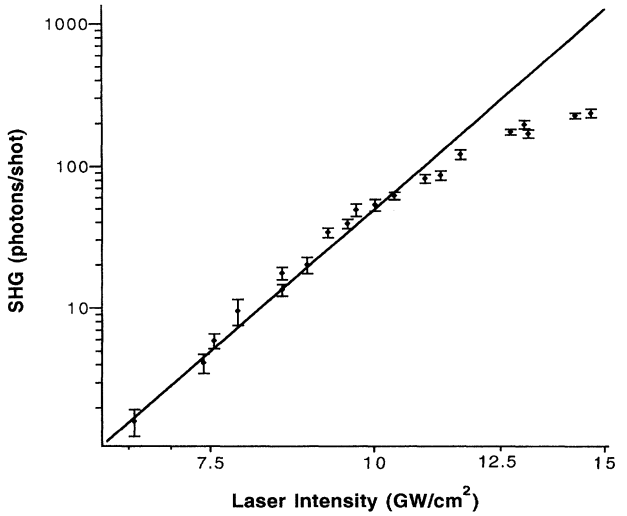

FIG. 1. Second harmonic signal as a function of pump intensity I. The straight line denotes an I^8 dependence.

out of the excitation region was then proportional to I^3. Since the SHG signal at low pump intensities should be proportional to $|E_{dc}|^2 I^2$, we can readily explain the observed I^8 dependence for SHG. SHG was not instantaneous, but relied on the overlap of the buildup curve of $E_{dc}(r,t)$ and the decay curve of the coherent excitation $\rho_{fg}(r,t)$, where r is the radial coordinate in the cylindrical coordinate system. A higher Ar pressure would slow down the buildup of $E_{dc}(t)$ but accelerate the decay of $\rho_{fg}(r,t)$, thereby leading to a smaller SH signal. The observed spatial profile and polarization of the SH output also appear to be characteristic of the ionization-initiated dc-field-induced SHG model predicted earlier by Bethune for the steady-state case [5].

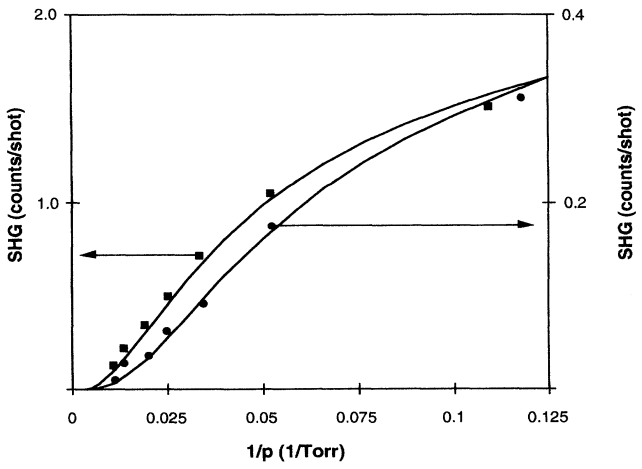

FIG. 2. Dependence of SHG on Ar pressure in 0.6 Torr potassium vapor with pump intensities at 14 GW/cm^2 (squares) and 8 GW/cm^2 (circles). The lines are obtained from theoretical calculations.

We now give a more quantitative description of the model. Assume an ultrashort pump pulse with a Gaussian profile and a peak intensity of 10^{10} W/cm^2. The free electrons released by three-photon ionization of K should have a radially symmetric initial density distribution of the form

$$N_e(r,0) = N\exp(-r^2/R_i^2), \tag{1}$$

which equals the initial ion density $N_i(r)$. We find from estimation $N \sim 1.3 \times 10^{11}$ cm^{-3}. Here, R_i is $1/\sqrt{3}$ times the pump beam radius due to three-photon ionization. The initial excess energy carried by each electron emancipated from three-photon ionization is 1.9 eV, corresponding to an initial velocity of $v_0 \sim 8 \times 10^5$ m/sec. In the Ar pressure ranges in which we are working, the electron motion is diffusive; however, thermalizing collisions with other electrons are rare, so the electrons maintain its initial velocity v_0 for a long time. Thus, after the pulsed ionization, electrons diffuse radially outward following the diffusive equation of motion,

$$\frac{\partial N_e(r,t)}{\partial t} = \nabla\cdot\left(\frac{v_0 L}{3}\nabla N_e(r,t) + \frac{eL}{v_0 m_e}N_e(r,t)\vec{E}_{dc}(r,t)\right), \tag{2}$$

where L is the mean free path of electrons, m_e is the mass of an electron, and E_{dc} is radially directed. The much slower ions are assumed to remain fixed. The dc field is obtained from Gauss' law,

$$E_{dc}(r,t) = \frac{4\pi e}{r}\int_0^r [N_i(r',0) - N_e(r',t)]r'\,dr'. \tag{3}$$

Knowing $N_i(r,0)$, $N_e(r,0)$, and v_0, we can find E_{dc} from Eqs. (2) and (3).

Because E_{dc} involves an integral of $N_e(r,t)$, the diffusion equation is nonlinear and this set of equations cannot be solved analytically. Numerical solution provides the details of the field evolution. E_{dc} grows until it balances the diffusive term in Eq. (2). For high levels of ionization, we find that the equilibrium electron density distribution $N_e(r,\infty)$ for $r < R_i$ is nearly equal to the original distribution $N_e(r,0)$, i.e., $N_e(r,\infty) = N_e(r,0) - \Delta$ with $N_e(r,0) \gg \Delta$. By setting Eq. (2) to zero, the equilibrium electric field becomes

$$\begin{aligned} E_{dc}(r) &= -\frac{v_0^2 m_e}{3e}\frac{(\partial/\partial r)[N_e(r,\infty)]}{N_e(r,\infty)} \\ &\approx -\frac{v_0^2 m_e}{3e}\frac{(\partial/\partial r)[N_e(r,0)]}{N_e(r,0)} = \frac{2v_0^2 m_e r}{3eR_i^2}. \end{aligned} \tag{4}$$

Note that this equilibrium form of E_{dc} is independent of $N_e(r,0)$. The approximation here is valid if $N_e(r,0) > 10^{11}/\text{cm}^3$.

The above result can be used to understand the different pump intensity dependence of SHG in nanosecond [3,4] and picosecond experiments. In both cases, the levels

of ionization were high enough for the approximation in Eq. (4) to work. However, it takes typically ~100 ps for E_{dc} to reach equilibrium. With the nanosecond pulse, $I(2\omega) \propto |E_{dc}|^2 I(\omega)^2 \propto I(\omega)^2$, since for most of the time duration of the pulse E_{dc} has already reached the constant equilibrium value given by Eq. (4) which does not depend on the input pump intensity or $N_e(r,0)$. With the picosecond pulse we probe the rising part of $E_{dc}(r,t)$ with the coherent excitation $\rho_{fg}(t)$ before E_{dc} approaches equilibrium. Since $E_{dc}(r,t)$ is proportional to $I(\omega)^3$ during the buildup, we find $I(2\omega) \propto I(\omega)^8$. Marmet, Hakuta, and Stoicheff [6] have also calculated the dc electric field created by the three-photon ionization of the hydrogen atom with a somewhat different model showing saturation of an average dc field.

The pump pulse also coherently excites a two-photon resonant transition, for example, $4s \rightarrow 9d$ of K. The effective perturbing Hamiltonian for a two-photon transition for the ground state atom is approximately [9]

$$\mathcal{H}_{\text{eff}} = \sum_{m \neq g} \frac{(eE)^2 x|m\rangle\langle m|x}{\hbar(\omega - \omega_{mg})}, \tag{5}$$

where $|m\rangle$ is an intermediate state, and $\hbar\omega_{mg}$ is the energy difference between unperturbed m and g levels. If the pump pulse width T_L is much shorter than the dephasing time T_2 of the transition, then immediately after the pump pulse is over the coherent excitation between $|g\rangle$ and $|f\rangle$ is given by

$$\rho_{fg}(0) = \frac{i}{\hbar}\langle f|\mathcal{H}_{\text{eff}}|g\rangle T_L, \tag{6}$$

which is expected to decay due to dephasing and Doppler effects. At $t > 0$, we have [8]

$$\rho_{fg}(t) = \rho_{fg}(0)\exp\left(i\omega_{fg}t - \frac{t^2}{T_D^2} - \frac{t}{T_2}\right),$$

$$T_2 = \frac{1}{\sqrt{2}\,v\sigma N_{\text{Ar}}}, \qquad T_D = \sqrt{\frac{2Mc^2}{k_B T \omega_{fg}^2}}, \tag{7}$$

where T_2 is assumed to be dominated by collisions of K with Ar, v is the average thermal velocity of Ar as well as K, σ is the collision cross section of the excited $9d$ state potassium with Ar [8], N_{Ar} is the density of Ar, T_D = 190 ps is due to the Doppler effect on the $4s$-$9d$ transition of K, M is the mass of potassium, and T is the oven temperature (600 K). By symmetry, it is impossible for $\rho_{fg}(t)$ to generate a nonvanishing macroscopic polarization at $2\omega = \omega_{fg}$. However, in the presence of E_{dc}, it does lead to a dc-field-induced polarization,

$$P_{2\omega}(r,t) \cong \sum_{np} \frac{N_K e^2 \langle g|x|np\rangle\langle np|x|f\rangle}{\hbar(\omega_{np,g} - 2\omega)} E_{dc}(r,t)\rho_{fg}(r,t). \tag{8}$$

The generated SH signal is proportional to the square of $P_{2\omega}(r,t)$ and can be calculated if all the relevant parameters are known.

The matrix elements in Eqs. (5) and (8) are known up to $n = 12$ from Eichner [10]. All the values in the equations

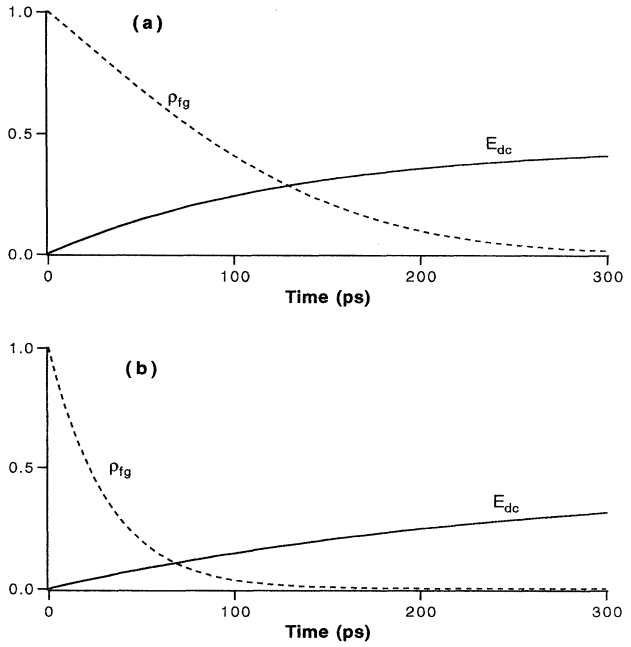

FIG. 3. Time development of E_{dc} (solid curve) and ρ_{fg} (dashed curve) for (a) 10 Torr and (b) 50 Torr of Ar pressure at $I(\omega) = 10$ GW/cm^2 and $r = 200$ μm.

are either known or can be evaluated. We have calculated $E_{dc}(r,t)$ and $\rho_{fg}(r,t)$ for different pump intensities and Ar pressures with K pressure kept at 0.6 Torr. Figure 3 gives two cases with different Ar pressures as examples. As expected, the higher Ar pressure results in less overlap between $E_{dc}(t)$ and $\rho_{fg}(t)$, and hence a weaker SHG. A full calculation of SHG versus Ar pressure is presented in Fig. 2 in comparison with the experimental data for two different intensities of the laser. At the higher laser intensity, E_{dc} reaches the equilibrium value in a time that is fast compared to either T_2 or T_D regardless of the Ar pressure, and SHG decreases with the Ar pressure mainly due to shortening of the coherent decay, $\rho_{fg} \propto e^{-t/T_2} \propto e^{-\alpha t P_{\text{Ar}}}$ where α is a constant. In this case, we have SHG $\propto \int_0^\infty |\rho_{fg}(t')|^2 dt'$, so we can expect a $1/P_{\text{Ar}}$ dependence of SHG. At the lower intensity where the buildup time of E_{dc} is comparable with T_2 or T_D, increasing the Ar pressure decreases the SHG in two ways. First SHG is reduced by the faster decay of ρ_{fg} with the higher Ar pressure as in the high intensity case. Second, as the tail of ρ_{fg} shrinks with the higher Ar pressure, it samples the earlier part and hence the weaker part of $E_{dc}(t)$ in the buildup. Altogether we expect a smaller SHG signal that is different from $1/P_{\text{Ar}}$ in the high pump intensity case. The solid lines in Fig. 2 are obtained from numerical simulation. They appear to describe the experimental data very well.

We can also employ a pump-probe scheme to test the model. The picosecond pump and probe pulses are used to create $E_{dc}(r,t)$ and $\rho_{fg}(r,t)$ separately. By varying the

time delay between two pulses, the time overlap between $E_{dc}(t)$ and $\rho_{fg}(t)$ can be adjusted and the SHG signal changes accordingly. The SH signal as a function of the time delay can be estimated from the equations given earlier. In the experiment, we arrange to have the pump and probe beams cross at the center of the cell at a small angle of 0.2°. The probe pulse had an intensity of ~3 GW/cm^2 and was not strong enough to generate a detectable SH signal by itself. With the pump pulse present, however, SHG by the probe pulse was readily observed. It was proportional to the square, instead of the eighth power, of the probe intensity. The result of SHG as a function of the pump-probe delay is displayed in Fig. 4 together with the theoretical calculation. It is seen that if the probe pulse is too far ahead of the pump pulse (negative time delay), the signal is negligibly small. As the two pulses get closer, $\rho_{fg}(t)$ generated by the probe overlaps with $E_{dc}(t)$ generated by the pump, and the dc-field-induced SHG becomes increasingly strong. Eventually, for sufficiently long positive time delays, $\rho_{fg}(t)$ moves completely under the saturated region of $E_{dc}(t)$, and the SH signal saturates accordingly. The signal remains nearly unchanged between delays of 100 and 600 ps, the limit of the setup. In Fig. 4, the results for pump intensities of 12 and 8 GW/cm^2 are shown. The higher pump intensity is expected to bring $E_{dc}(t)$ more rapidly to its saturation value. This is indeed reflected in the faster growth of the SH signal to saturation. As seen in Fig. 4, the agreement between theory and experiment is quite satisfactory, considering the simplicity of the model. The observed bump between delay times of 10 and 100 ps was not reproduced in the theoretical curve. This could be due to the fact that we have neglected the nondiffusive aspect of the electron motion during the initial period right after the electrons are released from the excitation region.

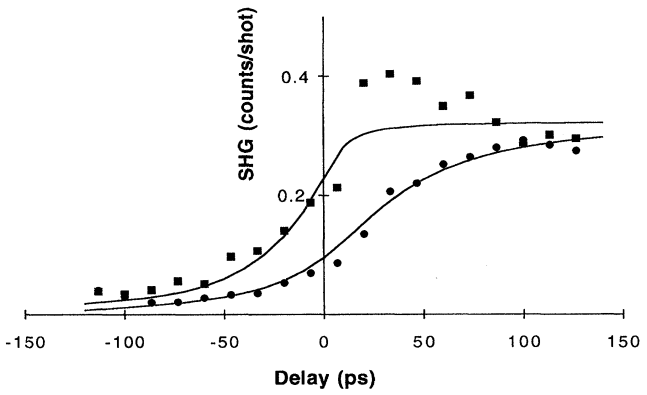

FIG. 4 SHG generated by the probe pulse as a function of time delay between the pump and probe pulses. Squares: pump intensity at 12 GW/cm^2. Circles: pump intensity at 8 GW/cm^2. The lines are theoretical fits. The buildup time of E_{dc} is ~30 ps (upper curve) and ~150 ps (lower curve).

In summary, we have studied two-photon resonant SHG in K/Ar vapor with picosecond laser pulses. We show that the ionization-initiated dc-field-induced SHG is the mechanism responsible for the observed resonant SHG. Because the laser pulse is short, the temporal buildup of the dc field and the decay of the two-photon coherent excitation must be taken into account. Our experiment is probably the first example of a transient two-photon coherent transient excitation that is forbidden to radiate but made allowed by the switch on of a dc field. A theoretical calculation reproduces all the characteristic features of the observation.

We would like to acknowledge help from J. Y. Zhang and H. T. Zhou on the project. This work was supported by the Director, Office of Energy Research, Office of Basic Energy Sciences, Materials Science Division of the U.S. Department of Energy under Contract No. DEA-AC03-76SF00098.

[1] See, for example, Y. R. Shen, *The Principles of Nonlinear Optics* (John Wiley & Sons, New York, 1984), p. 28.
[2] D. L. Andrews, J. Phys. B **13**, 4091 (1980); T. F. Heinz and D. P. DiVincenzo, Phys. Rev. A **42**, 6249 (1990).
[3] T. Mossberg, A. Flusberg, and S. R. Hartmann, Opt. Commun. **25**, 121 (1978); J. Okada, Y. Fukuda, and M. Matsuoka, J. Phys. Soc. Jpn. **50**, 1301 (1981); J. Bokor, R. R. Freeman, R. L. Panock, and J. C. White, Opt. Lett. **6**, 182 (1981); W. Jamroz, P. E. LaRocque, and B. P. Stoicheff, *ibid.* **7**, 148 (1982).
[4] S. Dinev, J. Phys. B **21**, 1681 (1988); M. Lu and J. Tsai, *ibid.* **23**, 921 (1990).
[5] D. S. Bethune, Phys. Rev. A **23**, 3139 (1981).
[6] L. Marmet, K. Hakuta, and B. P. Stoicheff, Opt. Lett. **16**, 261 (1991); L. Marmet, K. Hakuta, and B. P. Stoicheff, J. Opt. Soc. Am. B **9**, 1038 (1992).
[7] K. Miyazaki, T. Sato, and H. Kashiwagi, Phys. Rev. Lett. **43**, 1154 (1979); M. S. Malcuit, R. W. Boyd, W. V. Davis, and K. Rzążewski, Phys. Rev. A **41**, 3822 (1990); S. Augst, D. D. Meyerhofer, C. I. Moore, and J. Peatross, Proc. SPIE Int. Soc. Opt. Eng. **1229**, 152 (1990).
[8] T. F. Gallagher, S. A. Edelstein, and R. M. Hill, Phys. Rev. A **15**, 1945 (1977); A. Flusberg, R. Kachru, T. Mossberg, and S. R. Hartmann, *ibid.* **19**, 1607 (1979).
[9] D. Grischkowsky, M. M. T. Loy, and P. F. Liao, Phys. Rev. A **12**, 2514 (1975).
[10] H. Eichner, IEEE J. Quantum Electron. **QE-11**, 121 (1975).